BJP British Journal of Pharmacology

DOI:10.1111/j.1476-5381.2011.01374.x
www.brjpharmacol.org

RESEARCH PAPER

Distinct pharmacological and functional properties of NMDA receptors in mouse cortical astrocytes

Oleg Palygin[1], Ulyana Lalo[2] and Yuriy Pankratov[1]

[1]*Department of Biological Sciences, University of Warwick, Coventry, UK, and* [2]*Cell Physiology and Pharmacology, University of Leicester, Leicester, UK*

Correspondence
Dr Yuriy Pankratov, Department of Biological Sciences, University of Warwick, Coventry, CV4 7AL, UK. E-mail: y.pankratov@warwick.ac.uk

Keywords
Memantine; UBP141; NMDA receptor; GluN3A subunit; calcium permeability; neuron-glia communication; GluN3B; mouse cortex

Received
17 September 2010
Revised
15 February 2011
Accepted
11 March 2011

BACKGROUND AND PURPOSE

Astrocytes of the mouse neocortex express functional NMDA receptors, which are not blocked by Mg^{2+} ions. However, the pharmacological profile of glial NMDA receptors and their subunit composition is far from complete.

EXPERIMENTAL APPROACH

We tested the sensitivity of NMDA receptor-mediated currents to the novel GluN2C/D subunit-selective antagonist UBP141 in mouse cortical astrocytes and neurons. We also examined the effect of memantine, an antagonist that has substantially different affinities for GluN2A/B and GluN2C/D-containing receptors in physiological concentrations of extracellular Mg^{2+}.

KEY RESULTS

UBP141 had a strong inhibitory action on NMDA receptor-mediated transmembrane currents in the cortical layer II/III astrocytes with an IC_{50} of 2.29 μM and a modest inhibitory action on NMDA-responses in the pyramidal neurons with IC_{50} of 19.8 μM. Astroglial and neuronal NMDA receptors exhibited different sensitivities to memantine with IC_{50} values of 2.19 and 10.8 μM, respectively. Consistent with pharmacological differences between astroglial and neuronal NMDA receptors, NMDA receptors in astrocytes showed lower Ca^{2+} permeability than neuronal receptors with P_{Ca}/P_{Na} ratio of 3.4.

CONCLUSIONS AND IMPLICATIONS

The biophysical and pharmacological properties of the astrocytic NMDA receptors strongly suggest that they have a tri-heteromeric structure composed of GluN1, GluN2C/D and GluN3 subunits. The substantial difference between astroglial and neuronal NMDA receptors in their sensitivity to UBP141 and memantine may enable selective modulation of astrocytic signalling that could be very helpful for elucidating the mechanisms of neuron-glia communications. Our results may also provide the basis for the development of novel therapeutic agents specifically targeting glial signalling.

Abbreviations

DL-TBOA, DL-threo-b-benzyloxyaspartic acid; GSC, glial synaptic current; GFAP, glial fibrillary acidic protein; PPADS, pyridoxalphosphate-6-azophenyl-2′,4′-disulphonic acid tetrasodium salt; TFB-TBOA, (3S)3[[3[[4(trifluoromethyl)benzoyl] amino]phenyl]methoxy]-L-aspartic acid; UBP141, (2*R**,3*S**)-1-(phenanthrenyl-3-carbonyl)piperazine-2,3-dicarboxylic acid

Introduction

NMDA receptors are the most complex glutamate-gated ionotropic receptors in the CNS. They play a key role in the excitatory synaptic transmission and many brain functions, such as memory and cognition. NMDA receptors attract a great deal of interest in therapeutic research because of their involvement in various brain pathologies, including ischaemia, neurodegenerative and neuropsychiatric disorders, (Lipton, 2006; Paoletti and Neyton, 2007).

There is a great diversity in the NMDAR subtypes. It is widely accepted that functional NMDARs are tetrameric complexes assembled of the two obligatory GluN1 subunits, combined with one or two GluN2(A,B,CD) and/or GluN3(A,B)

subunits (Matsuda *et al*., 2003; Furukawa *et al*., 2005; Paoletti and Neyton, 2007). Subunit composition determines specific pharmacological and biophysical properties of these receptors, such as glutamate affinity, receptor desensitization, pharmacological sensitivity and channel block by extracellular Mg^{2+} (Cull-Candy and Leszkiewicz, 2004; Paoletti and Neyton, 2007). GluN2 and GluN3 subunit expression exhibits regional specificity and undergoes developmental regulation (Monyer *et al*., 1994; Cull-Candy and Leszkiewicz, 2004; Paoletti and Neyton, 2007; Henson *et al*., 2010).

Until recently, attention has been focused on the role of NMDA receptors in neuronal function and the functional expression of NMDA receptors in glia was not thought to be important. This is partly because of the voltage-dependent Mg^{2+} block, which suggested that NMDA receptors would be inactive at physiological resting potential in non-excitable glial cells. However, it has recently been reported that glial cells, namely oligodendrocytes (Karadottir *et al*., 2005; Micu *et al*., 2006) and cortical astrocytes (Lalo *et al*., 2006), express functional NMDA receptors that have distinct biophysical properties and may be composed of subunits that are different from GluN2A and GluN2B. Most importantly, glial NMDARs exhibit the weak Mg^{2+} block at physiological concentrations (Karadottir *et al*., 2005; Lalo *et al*., 2006) and therefore, can be active even at resting membrane potential. We have previously shown that astroglial NMDA receptors mediate transmembrane currents in cortical astrocytes that are activated upon physiological synaptic transmission (Lalo *et al*., 2006).

Recent studies linking glial NMDA receptors to various neurological disorders have ignited an interest in them as promising targets for the development of new therapeutic agents (Lipton, 2006; Matute *et al*., 2006). Finding specific antagonists of astroglial NMDAR receptors could allow the selective modulation of astroglial signalling without directly affecting neurons. This would be very useful for the investigation of the mechanisms of astroglial modulation of synaptic transmission and plasticity. However, the detailed pharmacological profile of glial NMDA receptors is far from complete. Hence, in this study we tested the sensitivity of mouse astroglial NMDA receptors to the novel antagonist UBP141, which has been reported to exhibit selectivity for the different GluN2 subunits (Morley *et al*., 2005; Brothwell *et al*., 2008). We also tested the action of memantine, an antagonist that is used therapeutically and has been reported to have a substantially different affinity for GluN2A/B and GluN2C/D-containing receptors at physiological concentrations of extracellular Mg^{2+} (Kotermanski and Johnson, 2009).

Methods

Slice and cell preparation

Experiments were performed on transgenic mice expressing enhanced green fluorescent protein (EGFP) under the control of the human glial fibrillary acidic protein (GFAP) promoter [line TgN(GFAP-EGFP)GFEC-FKi; see Nolte *et al*. 2001; Lalo *et al*. 2006]. Mice (4–8 weeks old) were anaesthetized with halothane (1.5–1.8 vol %) and then decapitated, in accordance with UK legislation. Slices were prepared using the technique described previously (Lalo *et al*., 2006). Brains were rapidly dissected in physiological saline containing (in mM): 135 NaCl, 3 KCl, 3 $MgCl_2$, 0.5 $CaCl_2$, 26 $NaHCO_3$, 1 NaH_2PO_4, 15 glucose, pH 7.4 when gassed with 95% O_2/5%CO_2. Brain slices (280–300 μm thick) were cut at 4°C, and were kept at room temperature for 1–4 h prior to *in situ* recordings and cell isolation in the above solution, but with (mM) $CaCl_2$ 2.5, $MgCl_2$ 1. The same extracellular solution was used for recordings in slices.

Astrocytes and neurons were acutely isolated from somatosensory cortex layer II/III using the modified 'vibrating ball' technique (Pankratov *et al*., 2002; Lalo *et al*., 2006). The glass ball (200 μm diameter) was moved slowly some 10–50 μm above the slice surface, while vibrating at 100 Hz (lateral displacements 20–30 μm). The composition of external solution for isolated cell experiments was (mM): 135 NaCl, 2.7 KCl, 2 $CaCl_2$, 1 $MgCl_2$, 10 HEPES, 1 NaH_2PO_4, 15 glucose; pH adjusted with NaOH to 7.3. In some experiments, the extracellular $CaCl_2$ concentration was elevated to 20 mM.

Electrophysiology

Cells were initially identified by size and the shape of somata under infrared gradient contrast and green fluorescence (astrocytes). After the whole-cell recording configuration had been established, identification of cells was verified by their response to a series of depolarizing and hyperpolarizing voltage steps from a holding potential of –80 mV (Lalo *et al*., 2006). All cells identified visually by EGFP fluorescence demonstrated an electrophysiological signature characteristic of astrocytes, that is, a series of passive currents with nearly linear I–V relationship, whereas cells identified as pyramidal neurons exhibited prominent rapidly activating currents elicited by depolarization, as described previously in Lalo *et al*. (2006).

Whole-cell voltage clamp recordings from the cortical astrocytes and pyramidal neurons were made with patch pipettes (5–6 MΩ) filled with intracellular solution (in mM): 110 KCl, 12 NaCl, 10 HEPES, 5 MgATP, 0.2 EGTA, pH 7.35. The membrane potential was clamped at –80 mV in the astrocytes and at –40 mV in the neurons, unless stated otherwise. Currents were monitored using an AxoPatch200B patch-clamp amplifier (Axon Instruments, Sunnyvale, CA, USA) filtered at 2 kHz and digitized at 4 kHz. Experiments were controlled by PCI-6229 data acquisition board (National Instruments, Austin, TX, USA) and WinFluor software (Strathclyde Electrophysiology Software, Glasgow, UK); data were analysed by custom-designed software.

Liquid junction potentials were measured with the patch-clamp amplifier; all voltages reported were corrected accordingly. Series resistances were 5–12 MΩ and input resistances were 50–150 MΩ for astrocytes and 400–900 MΩ for neurons; both varied by less than 20% in the cells accepted for analysis. A modified 'square-pulse' concentration jump method (Pankratov *et al*., 2002; Lalo *et al*., 2006) was used for rapid applications of solutions containing various agents to the acutely isolated cells. Unless stated otherwise, transmembrane currents were evoked in acutely isolated cortical neurons and astrocytes by the application of 50 μM NMDA and 1 μM glycine. Antagonists of NMDA receptors were pre-applied for 2 min before application of agonist. Between agonist applications, cells were constantly perfused with agonist-free extracellular solution using gravity-fed bath

application (flow rate 1–1.5 mL·min^{-1}). Responses of the cortical neurons and astrocytes to glycine were recorded in the presence of 10 μM strychnine and 100 μM picrotoxin.

To examine the synaptic currents *in situ*, voltage-clamp recordings were made from identified astrocytes and pyramidal neurons situated in the somatosensory cortex layer II/III at a temperature of 30–32°C. Axons originating from layer IV–VI neurons were stimulated at 0.15 Hz with a bipolar coaxial electrode (World Precision Instruments, Sarasota, FL, USA) placed in layer IV, approximately opposite the site of recording. Stimuli were single pulses (300 μs) with the magnitude adjusted to produce a synaptic current in neurons that was 30–40% of the maximal response (typically, stimulus amplitude was 5–7 μA). At such stimulus strength, the amplitude of the response in the astrocytes reached 25–30% of maximal.

To isolate the NMDA receptor-mediated components of glial and neuronal currents activated by synaptic stimulation, cortical slices were treated with the following pharmacological agents: picrotoxin 100 μM, a combination of the inhibitors of glutamate transporters (Danbolt, 2001; Hu *et al.*, 2003), (3*S*)-3-[[3-[[4-(trifluoromethyl)benzoyl]amino] phenyl]methoxy]-L-aspartic acid (TFB-TBOA, 1 μM) and DL-threo-b-benzyloxyaspartic acid (DL-TBOA, 30 μM); an antagonist of AMPA receptors, 6-cyano-7-nitroquinoxaline-2,3-dione (CNQX, 50 μM); the P2X receptor antagonist pyridoxalphosphate-6-azophenyl-2′,4′-disulphonic acid tetrasodium salt (PPADS, 30 μM). According to our previous reports (Lalo *et al.*, 2006; 2008), these concentrations of antagonists effectively inhibited P2X, AMPA receptors and glutamate transporters expressed in the cortical astrocytes and neurons.

Fluorescent Ca^{2+} imaging

To monitor intracellular Ca^{2+}, cortical astrocytes were loaded with 150 μM Fluo-3 through the whole-cell patch-pipette (substituting the EGTA in the intracellular saline). Cells were illuminated at 495 nm using the OptoScan monochromator (Cairn, UK); fluorescence was measured at 530 ± 20 nm.

The fluorescent images were recorded using an Olympus BX51 microscope (Olympus, Tokyo, Japan) with an UMPLFL20X/NA0.95 objective and 2× intermediate magnification and an iXon885 EMCCD camera (Andor Technology, Belfast, UK); exposure time was 35 ms at 2 × 2 binning. Elevation in the intracellular Ca^{2+} level was evaluated by $\Delta F/F_0$ ratio after background subtraction.

Data analysis

Data on the concentration-dependence of the effects of antagonists were fitted with the following: $I/I_0 = 1/(1 + ([B]/IC_{50})^{nH})$, where I is the current measured with drug concentration $[B]$, I_0 is the current in control conditions and n_H is the Hill coefficient. The relative calcium permeability of NMDA receptors was calculated from the reversal potential of NMDA-activated current in the context of the extended Goldman–Hodgkin–Katz theory as described previously (Lewis, 1979; Mayer and Westbrook, 1987; Pankratov *et al.*, 2002). Briefly, the current–voltage relationships of the NMDA responses were normalized to the amplitude at –40 mV, averaged over all cells and fitted with a polynomial curve to determine a reversal potential. The permeability ratios for Ca^{2+} to Na^+ (P_{Ca}/P_{Na}) and Na^+ to K^+ (P_{Na}/P_K) were calculated from values of reversal potential at two different extracellular calcium concentrations converted to the activities in the electrolyte solutions (Mayer and Westbrook, 1987; Castro and Albuquerque, 1995). The following activity coefficients were used: 0.77 for Na^+ and K^+, 0.29 and 0.26 for low and high concentrations of Ca^{2+}.

Drugs

UBP141 was purchased from Ascent Scientific (Bristol, UK); other receptor antagonists were from the Tocris Bioscience, and other salts and chemicals were from Sigma (Dorset, UK).

Results

Agonist-evoked currents in acutely isolated astrocytes and neurons

Recordings from visually identified acutely isolated fluorescent astrocytes were made within 20–50 min after isolation. Taking into account the competitive mechanism of UBP141 action (Morley *et al.*, 2005) we activated astrocytic NMDA receptors by addition of a saturating concentration of NMDA (50 μM, see Lalo *et al.*, 2006; Erreger *et al.*, 2007). Application of 50 μM NMDA with 1 μM glycine at a holding potential –80 mV (in 1 mM extracellular Mg^{2+}) evoked inward currents in all of 58 astrocytes tested (Figure 1A). The functional properties of the NMDA-activated currents, that is, slow desensitization kinetics, high affinity to agonist, sensitivity to D-AP5 and lack of Mg^{2+} block were similar to our data reported previously for cortical astrocytes (Lalo *et al.*, 2006, see also Figure 4A). In contrast to the astrocytes, L2/3 pyramidal neurons did not respond to NMDA at a holding potential of –80 mV due to Mg^{2+} block; currents elicited by NMDA in the pyramidal neurons at other holding potentials had functional properties very similar to NMDA receptors in hippocampal and cortical neurons (Mayer and Westbrook, 1987; Lalo *et al.*, 2006, see also Figure 4B). Unless stated otherwise, all experiments reported below were carried out at a holding potential of –80 mV in astrocytes and at –40 mV in neurons.

UBP141, novel subunit-selective antagonist of NMDA receptors, had different inhibitory effects on astrocytes and neurons (Figure 1). Pre-incubation with 3 μM UBP141 for 2 min decreased the amplitude of NMDA-evoked responses (Figure 1A) in the astrocytes by 62 ± 14% (n = 7) whereas neuronal responses (Figure 1B) were inhibited by only 9 ± 11% (n = 6). The effects of UBP141 were reversible in both the astrocytes and neurons. The inhibitory action of UBP141 on NMDA-activated currents in cortical astrocytes was concentration-dependent (Figure 1C) with an IC_{50} of 2.29 ± 0.37 μM (n = 7). The IC_{50} for glial NMDA receptors was close to the IC_{50} values reported for the action of UBP141 on GluN1/GluN2C- and GluN1/GluN2D receptor-mediated responses activated by a saturating concentration of the agonist (Morley *et al.*, 2005). The IC_{50} for the effect of UBP141 on NMDA responses recorded in neurons was 19.8 ± 3.4 μM (n = 6); this value closely agrees with IC_{50} values for GluN1/GluN2A and GluN1/GluN2B receptors (Morley *et al.*, 2005).

We also tested the inhibitory action of ifenprodil, another subunit-selective NMDA receptor antagonist. Incubation

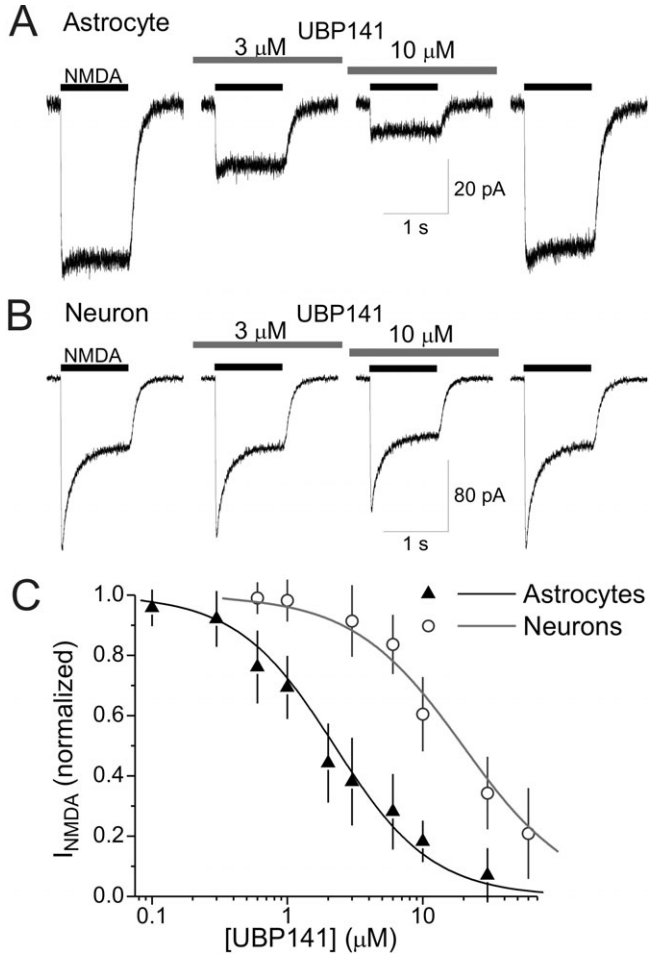

Figure 1

The GluN2C/D subunit-selective antagonist UBP141 differentially suppresses NMDA receptors in the astrocytes and neurons. (A) Representative traces illustrate the current activated by 50 μM NMDA in the acutely isolated cortical layer II/III astrocyte before and after application of 3 and 10 μM UBP141. (B) Effect of the same concentrations of UBP141 on current activated by 50 μM NMDA in a pyramidal neuron acutely isolated from the same cortical slice. Note the much weaker inhibitory effect of UBP141 in the neuron. (C) The mean concentration-dependent effect of UBP141 in seven astrocytes (IC_{50}, 2.29 ± 0.37 μM; Hill coefficient, 1.19 ± 0.14) and six neurons (IC_{50}, 19.8 ± 3.4 μM; Hill coefficient, 1.08 ± 0.15). The amplitude of the NMDA response was normalized to control. Error bars represent SD. Holding membrane potential was –80 mV in astrocytes and –40 mV in neurons.

with 10 μM ifenprodil did not significantly affect the amplitude of NMDA-activated currents in the cortical astrocytes (3 ± 7% decrease; n = 15, P > 0.05, one-population t-test; data not shown). In contrast, the same concentration of ifenprodil inhibited the NMDA response in cortical neurons by 58 ± 11% (n = 6, data not shown). The absence of a notable effect of ifenprodil on the NMDA response in the astrocytes indicates a low level (if any) expression of GluN2B subunits. This result is slightly different from our previous data (Lalo *et al.*, 2006) obtained in younger mice (17–22 days old), where we observed partial (less than 50%) inhibition of NMDA receptors by 10 μM ifenprodil in the sub-population (about 30%) of cortical astrocytes. The expression of both GluN2B and GluN2C subunits in cortical astrocytes obtained from younger mice has also been reported by Schipke *et al.* (2001). This variation in the subunit composition of astroglial NMDA receptors may be related to developmental changes; a decrease in the expression of GluN2B and an increase in the expression of GluN2C subunit have been reported in neurons with age (Henson *et al.*, 2010; Steinert *et al.*, 2010). Also, a pathologically-evoked expression of the GluN2B subunit has been shown to occur in astrocytes after ischaemic insults during tissue preparation (Krebs *et al.*, 2003).

The marked difference in the inhibitory action of UBP141 suggests a different subunit composition of NMDA receptors in cortical astrocytes and neurons. Astroglial NMDA receptors were thought to lack GluN2A and B subunits but contain GluN2C or D subunit. This hypothesis was supported by data on the inhibitory action of memantine (Figure 2). As the effects of memantine on NMDA receptors depend on membrane potential and extracellular Mg^{2+} concentration (Wrighton *et al.*, 2008; Kotermanski and Johnson, 2009), we measured the effect of memantine on astroglial and neuronal receptors at physiological Mg^{2+} concentrations and membrane potentials at which these receptors would probably be activated during physiological activity, correspondingly –80 mV and –40 mV. Pre-application of 1 μM and 10 μM memantine decreased the amplitude of NMDA-evoked currents in the astrocytes by 39 ± 12% and 72 ± 7%, respectively (n = 7) (Figure 2A). However, neuronal responses to NMDA were correspondingly inhibited by 7 ± 11% and 46 ± 10% (n = 6) (Figure 2B).

Memantine exhibited different affinities for glial and neuronal NMDA receptors (Figure 2C). The IC_{50} for the action of memantine on NMDA-evoked currents in the cortical astrocytes was 2.19 ± 0.18 μM (n = 7) at –80 mV and 4.24 ± 0.47 μM (n = 5) at –40 mV. The weak voltage-dependence of the effect of memantine on astroglial NMDA receptors was similar to its voltage-dependent effect on GluN2D receptors (Wrighton *et al.*, 2008). The IC_{50} for the action of memantine on NMDA receptors in the cortical neurons was 10.8 ± 0.55 μM (n = 6) at –40 mV. It should be noted that the IC_{50} value for NMDA-evoked currents in neurons obtained in our experiments is in very good agreement with the data of Kotermanski and Johnson (2009) on the affinity of memantine to GluN2A and B subunits (constituent subunits of the majority of neuronal NMDA receptors) at physiological concentrations of Mg^{2+}. Also, the IC_{50} for the effect of memantine on NMDA responses in astrocytes closely agrees with the sensitivity of GluN2C/D-containing receptors (Kotermanski and Johnson, 2009).

Synaptically activated currents in cortical astrocytes and neurons in situ

Results obtained in the acutely isolated cells were corroborated by data on the pharmacological sensitivity of NMDA receptor-mediated components of synaptic response in astrocytes and neurons in brain slices. We performed voltage-clamp recordings from protoplasmic astrocytes and pyramidal neurons in layer II/III of somatosensory cortex of EGFP/GFAP mice (Nolte *et al.*, 2001). The astrocytes in acutely prepared brain slices were identified by green

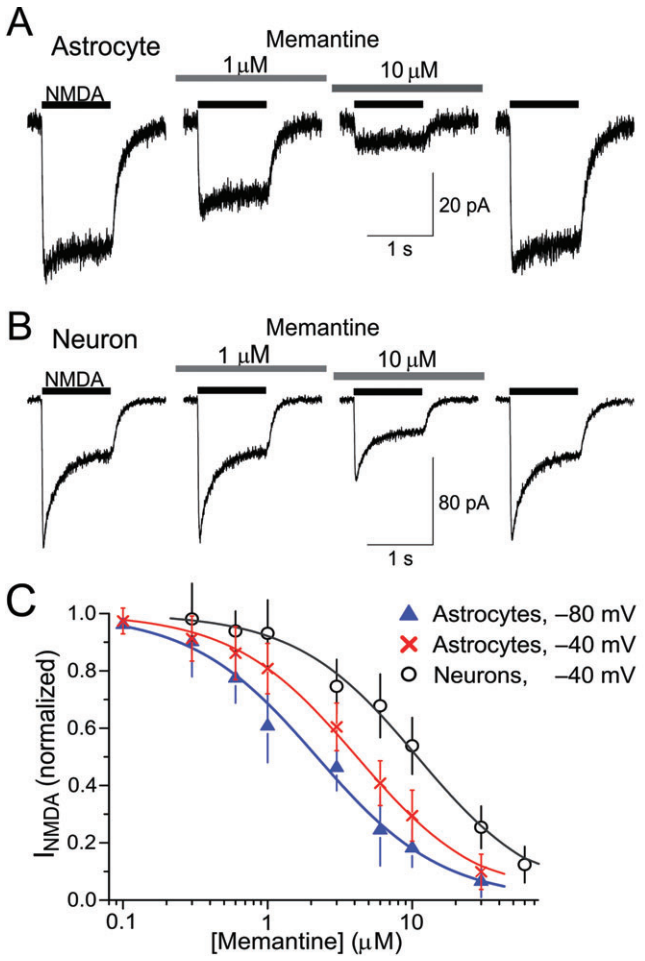

Figure 2

Memantine differentially inhibits NMDA receptors in astrocytes and neurons. (A) Representative traces illustrate the NMDA-activated current recorded in the acutely isolated cortical layer II/III astrocyte before and after application of 1 and 10 μM of memantine. (B) Effect of the same concentrations of memantine on an NMDA-activated current in a pyramidal neuron acutely isolated from the same cortical slice. Note the much weaker inhibitory effect of memantine in the neuron. (C) The mean concentration-dependent effect of memantine in seven astrocytes at –80 mV (IC_{50}, 2.19 ± 0.18 μM; Hill coefficient, 1.01 ± 0.07), in five astrocytes at –40 mV (IC_{50}, 4.24 ± 0.47 μM; Hill coefficient, 1.03 ± 0.11) and in six neurons at –40 mV (IC_{50}, 10.8 ± 0.55 μM; Hill coefficient, 1.04 ± 0.05). Error bars represent SD.

fluorescence and by their characteristic electrophysiological properties (see Methods).

Stimulation of neuronal afferents originating from layers IV–VI in the presence of 100 μM picrotoxin induced espcs in neurons and transmembrane ion currents in the astrocytes (Figure 3, see also Lalo *et al.*, 2006). Ion currents induced in the astrocytes were directly associated with synaptic transmission because (i) treatment of slices with 1 μM TTX completely abolished glial responses, (ii) the amplitude of the glial response was stimulus-dependent in a manner similar to the synaptic current evoked in the neighbouring neurons and (iii) the latency time of the glial responses was the same as the latency of the epscs (1.5–2.5 ms). Therefore, we identified astroglial responses as glial synaptic currents (GSCs). As has been shown previously (Lalo *et al.*, 2006), the major part of the cortical GSC was mediated by glial NMDA receptors and glutamate transporters. AMPA and P2X receptors can also participate in ionotropic signalling in cortical astrocytes (Lalo *et al.*, 2006; 2008). As we have discussed previously (Lalo *et al.*, 2006), astrocytic GSCs most likely result from both spill-out of neurotransmitter from cortical synapses and ectopic release, similar to Bergmann glial cells (Matsui and Jahr, 2004). Cortical astrocytes may also be a direct target of axon collaterals, like NG2+ glial cells in the hippocampus and cerebellum (Bergles *et al.*, 2009).

To isolate NMDA receptor-mediated synaptic responses, recordings were carried out in the presence of CNQX (30 μM), TFB-TBOA (1 μM), DL-TBOA (30 μM) and PPADS (30 μM). GSCs recorded under these conditions in astrocytes at –80 mV had a 10–90% rise time of 19.3 ± 4.2 ms and decay time of 690 ± 210 ms (n = 22); corresponding parameters of epscs recorded in neurons at –40 mV were 8.9 ± 2.7 ms and 148 ± 41 ms (n = 22). Application of 30 μM D-AP5 inhibited the astrocytic GSCs and neuronal epscs by 96 ± 7% and 93 ± 9%, respectively (n = 5, data not shown).

Similar to NMDA-activated currents in the acutely isolated cells, NMDA receptor-mediated synaptic responses in astrocytes and neurons *in situ* exhibited different sensitivities to UBP141, ifenprodil and memantine (Figure 3). Application of 3 μM UBP141 to cortical slices decreased the amplitude of astrocytic GSCs by 58 ± 6% (n = 9), which recovered after washout of UBP141. However, consecutive application of ifenprodil (10 μM) had no notable effect on astrocytic NMDA receptors (Figure 3A). In contrast, application of 3 μM UBP141 decreased the amplitude of neuronal epscs by only 8 ± 6%, whereas ifenprodil inhibited epscs by 63 ± 9% (n = 9).

The effects of memantine confirmed the different sensitivities of the astrocytic and neuronal responses to NMDA. Memantine (1 μM and 10 μM; Figure 3B) reversibly inhibited astrocytic GSCs by 41 ± 8% and 81 ± 6%, respectively (n = 8). However, 1 μM memantine had no effect on neuronal epscs (inhibition by 5 ± 6%; P > 0.05, one-population t-test), whereas 10 μM memantine inhibited these epscs by 49 ± 8% (n = 8).

Theoretically, changes in the extracellular potassium concentration due to activity of neuronal glutamate receptors might contribute to the inward current activated in the astrocytes by stimulation of synaptic pathways. To verify that the decrease in the GSC amplitude observed in the above experiments was due to inhibition of astrocytic NMDA receptors, we perfused cortical astrocytes with 10 μM MK801 through the patch-pipette and applied D-AP5, UBP141 and memantine in the bath solution. Blocking the astrocytic NMDA receptors with intracellular MK-801 caused a slow but strong inhibition of the GSCs recorded in the presence of 100 μM picrotoxin, 50 μM CNQX and 30 μM PPADS in all 10 cells tested (Figure 3C). Neither D-AP5 nor UBP141 had a notable effect (n = 6) on the residual GSCs resistant to intracellular MK-801; this residual current was almost completely abolished after application of the glutamate transporter blockers TFB-TBOA (1 μM) and DL-TBOA (30 μM). Similarly, memantine (10 μM) did not exhibit an inhibitory action on GSCs in

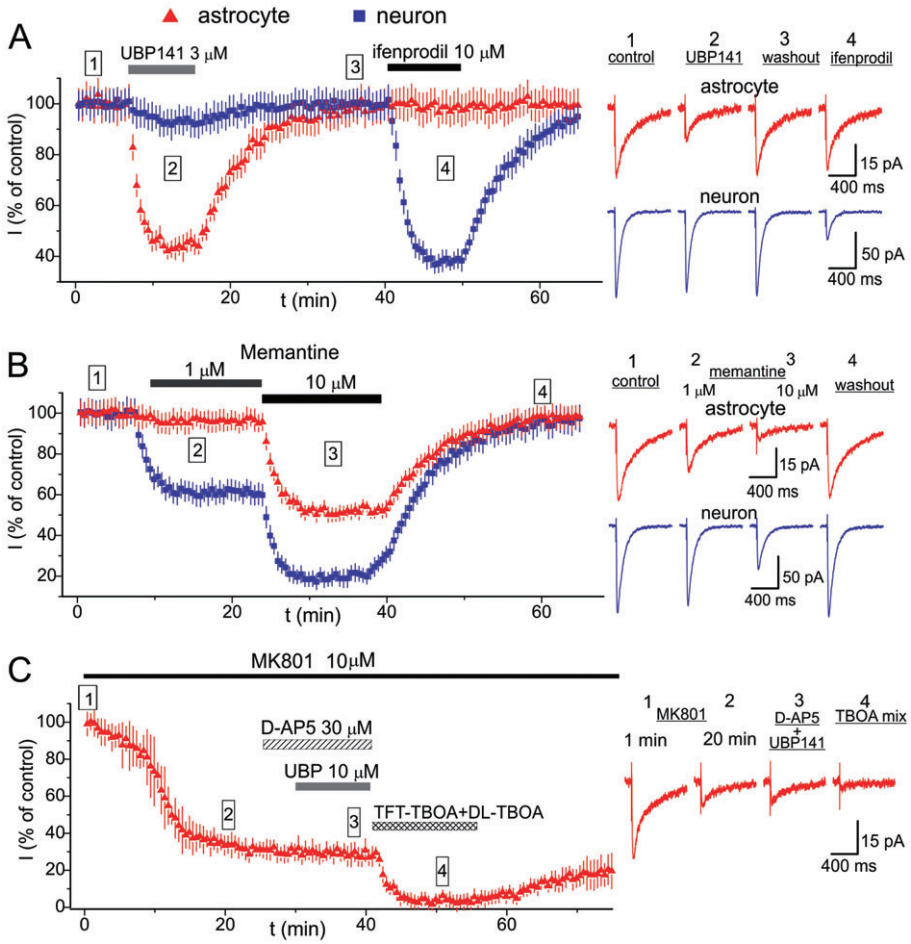

Figure 3

Effect of UBP141 and memantine on the NMDA-receptor mediated synaptic currents in astrocytes and neurons *in situ*. Transmembrane currents evoked in the astrocytes (glial synaptic currents; GSCs) and pyramidal neurons (epscs) of layer II/III of mouse neocortex *in situ* by stimulation of neuronal afferents were recorded in presence of 100 μM picrotoxin, 50 μM CNQX and 30 μM PPADS. (A) Left panel shows the changes in the amplitude of astrocytic GSCs and neuronal epscs following the bath application of 3 μM UBP141 and 10 μM ifenprodil. Data are presented as mean ± SD for 9 cells. (B) Changes in the astrocytic GSCs and neuronal epscs after application of 1 and 10 μM memantine (mean ± SD for eight cells). Data shown in (A) and (B) were measured in the constant presence of glutamate transporters antagonists TFB-TBOA, 1 μM and DL-TBOA, 30 μM. Each point in the time graphs shows the average amplitude (relative to control) of 5 sequential currents. Illustrative examples of GSCs and epscs (average of five traces) recorded as indicated, are shown in the right panels. Note the different inhibitory effects produced by UBP141, ifenprodil and memantine in the astrocytes and neurons. (C) Left panel shows the changes in the amplitude of astrocytic GSCs measured immediately after the establishment of whole-cell recording using intracellular solution supplemented with 10 μM MK-801 (mean ± SD for six cells). D-AP5, UBP141 and a combination of TFB-TBOA (1 μM) and DL-TBOA (30 μM) were applied to cortical slices as indicated. Note that UPB141 did not decrease the amplitude of the GSCs, when astrocytic NMDA receptors were inhibited by intracellular MK-801, confirming that its action shown in (A) was due to inhibition of glial NMDA receptors.

the presence of intracellular MK801 in all four astrocytes tested (data not shown).

These results confirm that the effects of UBP141 and memantine were due to direct inhibition of astrocytic NMDA receptors. The small residual GSC (2 ± 4%, $n = 10$) remaining in the presence of antagonists of NMDA receptors and glutamate transporters may, however, be associated with a redistribution of the extracellular potassium in the vicinity of the astroglial membrane.

It is worth noting that the inhibitory effects of UBP141 and memantine observed in the astrocytes and neurons *in situ* closely agree with data obtained in acutely isolated cells. Importantly, our results demonstrate the feasibility of selective pharmacological modulation of NMDA receptor-mediated signalling in neurons and astrocytes in physiological conditions.

Functional properties and subunit composition of astroglial NMDA receptors

The above results suggest incorporation of GluN2C/D subunits in NMDA receptors expressed in cortical astrocytes. Although GluN2C/D subunits have a lower affinity for Mg^{2+} than GluN2A/B, they are still blocked by physiological concentrations (>0.5 mM) of Mg^{2+} (Qian and Johnson, 2006). In

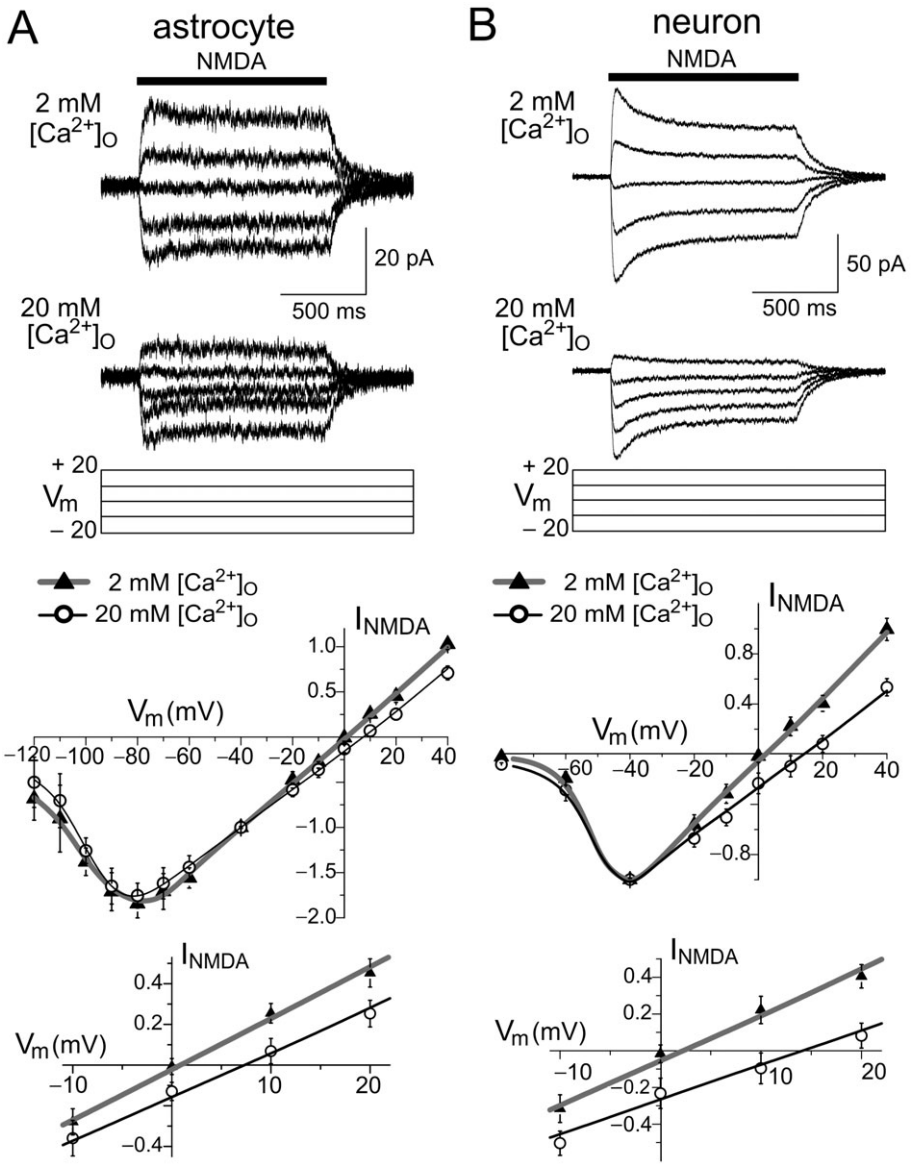

Figure 4

Voltage-dependence of the currents mediated by NMDA receptors in astrocytes and neurons. The upper panels show currents induced by rapid application of NMDA (50 μM, 1 s) recorded at the different holding potentials in a cortical astrocyte (A) and pyramidal neuron (B) in 2 and 20 mM extracellular Ca^{2+}. The lower panels show the *I–V* curves constructed from 11 (astrocytes) and 6 (neurons) independent experiments. The amplitudes of the responses to NMDA were normalized to the value measured at –40 mV; data are presented as mean ± SD. Solid lines show the results of a best polynomial fit (least squares routine), intersection with zero current axis gives the following values of reversal potential in 2 and 20 mM Ca^{2+}_{OUT}: 0.92 mV and 7.5 mV for astrocytes and 2.75 and 14.1 mV for neurons. The permeability ratio P_{Ca}/P_{Na} calculated in the framework of extended Goldman-Hodgkin–Katz equation is 3.4 for astrocytes and 7.5 for neurons.

contrast, NMDA receptors containing one or two GluN3 subunits were shown to have much lower sensitivity to Mg^{2+} block at physiological concentrations (Sasaki *et al.*, 2002; Tong *et al.*, 2008; Henson *et al.*, 2010). Incorporation of GluN3 subunits, however, would lower the calcium permeability of the NMDA receptors.

Taking into account the importance of Ca^{2+} signalling for the physiological activity of glial cells, we evaluated Ca^{2+} permeability of astroglial NMDA receptors using the Goldman–Hodgkin–Katz theory (see Methods). The reversal potential of NMDA-induced currents in the isolated cortical astrocytes in 2 and 20 mM extracellular Ca^{2+} was 0.92 ± 0.89 mV and 7.5 ± 2.4 mV ($n = 7$), respectively (Figure 4). The corresponding values for the neuronal NMDA-responses were 2.75 ± 0.97 mV and 14.1 ± 2.8 mV ($n = 6$). The permeability ratio P_{Ca}/P_{Na} calculated from the reversal potential of the NMDA-mediated current was 3.4 for astrocytes and 7.5 for neurons.

The P_{Ca}/P_{Na} ratio obtained for the NMDA receptors in cortical neurons agrees with data reported previously for neu-

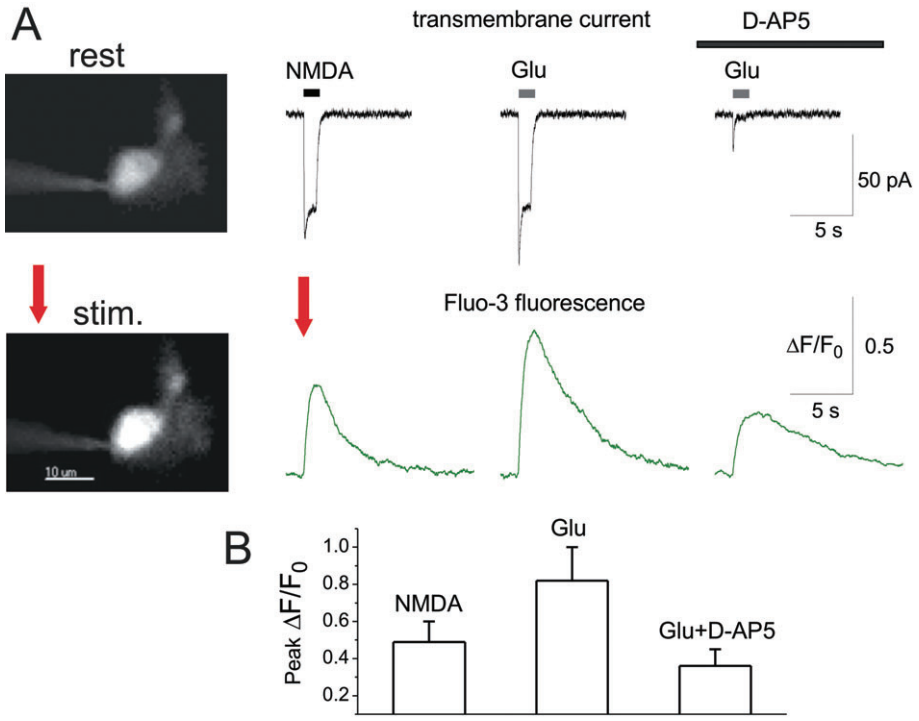

Figure 5

NMDA receptor-mediated Ca^{2+} signalling in cortical astrocytes. (A) An acutely isolated astrocyte was loaded with Fluo-3 via a somatic patch pipette. Fluorescent images were recorded simultaneously with transmembrane currents evoked by application of 20 μM NMDA and 100 μM glutamate in control and after consecutive application of 30 μM D-AP5. Representative images (left) and glial currents (right, upper row) were recorded before (rest) and after application of agonist. Ca^{2+} transients (right, lower row) represent the $\Delta F/F_0$ ratio averaged over the cell soma; scale bar is 10 μm. Holding potential is −80 mV. Transmembrane current activated by glutamate in control is mediated by NMDA and AMPA receptors and glutamate transporters. The NMDA-component was eliminated by D-AP5. The Ca^{2+} transient activated by glutamate in the control was mediated by metabotropic glutamate receptors, NMDA receptors and possibly by Ca^{2+}-permeable AMPA receptors. The Ca^{2+} transient activated by glutamate in the presence of D-AP5 lacks the NMDA-receptor-mediated component. (B) Pooled data (mean ± SD for five astrocytes) of peak Ca^{2+} transients; the difference is statistically significant with $^*P < 0.01$ and $^{**}P < 0.005$ (one-way ANOVA). Note the significant contribution made by the NMDA receptors to the glutamatergic Ca^{2+} signal in the astrocytes.

ronal NMDA receptors and various heterologously expressed GluN1/GluN2 subunit combinations (Mayer and Westbrook, 1987; Iino *et al.*, 1990; Matsuda *et al.*, 2003; Tong *et al.*, 2008). On the other hand, our evaluation of the relative Ca^{2+} permeability of astroglial NMDA receptors is very close to the results of recent studies of GluN3 subunit-containing receptors (Sasaki *et al.*, 2002; Matsuda *et al.*, 2003; Tong *et al.*, 2008). It should be noted that even though the Ca^{2+} permeability of astroglial NMDA receptors is lower than that of neuronal receptors, it is close to the permeability of other ionotropic receptors, like neuronal nicotinic ACh receptors ($P_{Ca}/P_{Na} \approx 2.1–6.1$) or P2X1 ($P_{Ca}/P_{Na} = 3.9$) and P2X2 ($P_{Ca}/P_{Na} = 2.2$) receptors (Castro and Albuquerque, 1995; Evans *et al.*, 1996; Fucile, 2004), and is larger than the permeability of Ca^{2+}-permeable kainate ($P_{Ca}/P_{Na}=0.74$) and AMPA ($P_{Ca}/P_{Na} \approx 0.5–1.7$) receptors (Burnashev *et al.*, 1996; Isa *et al.*, 1996).

To verify that astroglial NMDA receptors can contribute to Ca^{2+} signalling, we measured the elevation in the cytosolic Ca^{2+} level simultaneously with transmembrane currents induced by application of glutamate and NMDA to the isolated cortical astrocytes (Figure 5). Both NMDA and glutamate triggered a significant rise in the intracellular Ca^{2+} in the astrocytes. The amplitude of the NMDA-induced Ca^{2+} transients reached 56.8 ± 13.1 % ($n = 5$) of Ca^{2+} transients activated by glutamate, whereas the amplitudes of NMDA-activated and glutamate-activated transmembrane currents were almost similar. Application of 30 μM D-AP5 decreased the magnitude of the glutamate-activated Ca^{2+} transients (Figure 5) by 54.1 ± 10.9% ($n = 5$) and inhibited the transmembrane current even more strongly (89.4 ± 12.3%, $n = 5$); transmembrane currents were eliminated by further application of 30 μM NBQX (data not shown). These observations clearly indicate that a substantial component of the glutamatergic Ca^{2+} signalling in cortical astrocytes is independent of NMDA receptors. This component is most likely to be mediated by metabotropic glutamate receptors, which have been widely reported to participate in the astroglial Ca^{2+} signalling (Agulhon *et al.*, 2008). Our data also show that astroglial NMDA receptors, by virtue of their Ca^{2+} permeability and weak Mg^{2+} block, are capable of delivering significant Ca^{2+} influx in cortical astrocytes. One could estimate the contribution of NMDA receptors to the Ca^{2+} transients elicited by glutamate as 50–55%.

The combination of the lack of Mg^{2+} block together with lower Ca^{2+} permeability strongly suggests the presence of the GluN3 subunit in glial NMDARs. Accordingly, the expression

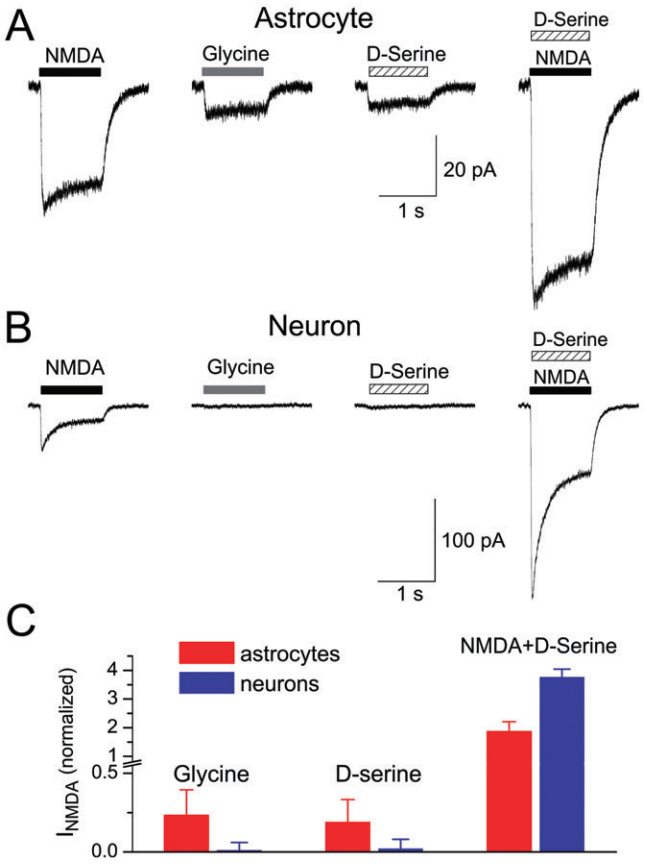

Figure 6

Effect of glycine and D-serine on astroglial and neuronal NMDA receptors. (A, B) Representative responses activated in acutely-isolated cortical astrocyte and neuron by consecutive application of 50 μM NMDA (no glycine added), 10 μM glycine, 10 μM D-serine and 20 μM NMDA and D-serine together. (C) Pooled data (mean ± SD for 10 astrocytes and 7 neurons) of amplitude of current activated by glycine, D-serine and NMDA and D-serine together; amplitudes were normalized to the amplitude of the NMDA-activated current. Recordings were made at a holding potential of –80 mV in the astrocytes and –40 mV in the neurons. Note the weak agonist action of glycine and D-serine in the astrocytes.

of pure di-heteromeric GluN1/GluN3 receptors in cortical astrocytes cannot be ruled out *a priori*. The most characteristic property of such receptors is an ability to be activated by glycine or D-serine in the absence of glutamate. We found that glycine and D-serine acted as weak agonists, inducing inward currents of much smaller amplitude than currents induced by NMDA or glutamate, in all 10 astrocytes tested (Figure 6). This contrasts with the much higher potency of glycine that one would expect of pure GluN1/GluN3 receptors (Chatterton *et al.*, 2002; Henson *et al.*, 2010). We also observed potentiation of NMDA-activated currents in astrocytes by 10 μM D-serine (Figure 6), this is in contrast to the D-serine-induced desensitization of GluN1/GluN3 receptors reported previously (Chatterton *et al.*, 2002). On the other hand, a partial agonist action of glycine on the cortical astrocytes closely agrees with data reported for GluN1/ GluN2A/ GluN3B tri-heteromeric receptors (Cavara and Hollmann, 2008).

To elucidate whether currents activated in the cortical astrocytes by glycine and D-serine were mediated by di-heteromeric or tri-heteromeric receptors, we tested their sensitivity to NMDA receptor antagonists. Weak block by classic NMDA antagonists is a characteristic feature of GluN1/GluN3 receptors, whereas triplet GluN1/GluN2/GluN3 receptors can be blocked by antagonists targeting GluN2 subunits (Sasaki *et al.*, 2002; Smothers and Woodward, 2009; Henson *et al.*, 2010). MK-801 (10 μM), memantine (10 μM) and UBP141 (10 μM) strongly inhibited the response of astrocytes to glycine (Figure 7A) and D-serine (Figure 7B). The inhibitory effects of the NMDA receptor antagonists on glycine and D-serine-activated currents in the astrocytes did not differ significantly from their action on NMDA-activated currents (Figure 7C), indicating that di-heteromeric GluN1/GluN3 receptors contribute little to glutamatergic signalling in cortical astrocytes. Taken together, our results suggest that NMDA receptors in cortical astroglia are assembled from GluN1, GluN2 and GluN3 subunits.

Discussion

Our results demonstrate striking differences in the properties of astrocytic and neuronal NMDA receptors. Moreover, our findings provide several clues to identify the subunit composition of astroglial NMDA receptors. There is no doubt that glial NMDA receptors contain two GluN1 subunits that are essential for trafficking to the membrane (Matsuda *et al.*, 2003; Furukawa *et al.*, 2005). In di- and tri-heteromeric NMDA receptors, expression of certain types of GluN2A-D subunits confers sensitivity to selective antagonists, such as D-AP5 or ifenprodil (Paoletti and Neyton, 2007). Hence, the most feasible explanation for the high affinity of astroglial receptors to UBP141 and memantine, and their low sensitivity to ifenprodil is their incorporation of GluN2C or GluN2D subunits. This hypothesis is also corroborated by very high potency of glutamate and NMDA in astroglial NMDA receptors (Lalo *et al.*, 2006), which is close to the data reported for recombinant GluN1/GluN2D receptors (Erreger *et al.*, 2007).

At the same time, glial NMDA receptors have a very low sensitivity to Mg^{2+} block, as shown previously bt Lalo *et al.* (2006), and was confirmed again in our present experiments. The GluN3 subunit is the only type of NMDA subunit that is not sensitive to physiological concentrations of Mg^{2+}. However, the stoichiometry of astroglial NMDA receptors might be different, with incorporation of either one or two GluN3 subunits (Henson *et al.*, 2010). The functional expression of GluN1/GluN3 di-heteromeric receptors has been suggested for cerebrocortical neurons (Chatterton *et al.*, 2002) and white matter oligodendrocytes have been shown to express tri-heteromeric receptors (Karadottir *et al.*, 2005; Burzomato *et al.*, 2010).

The most peculiar feature of di-heteromeric GluN1/GluN3 receptors is their ability to be activated by glycine and, arguably, D-serine with higher potency than glutamate; this has even given rise to their alternative name 'excitatory glycine receptors' (Chatterton *et al.*, 2002). However, these properties do not accord with our observations: glycine and D-serine were not found to be highly potent activators of the inward currents in the cortical astrocytes (Figure 6). We observed

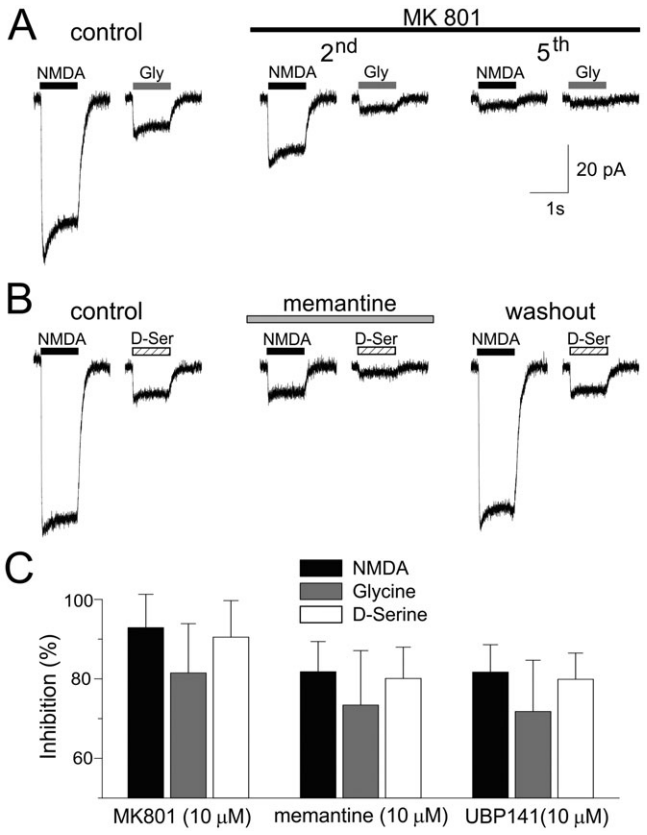

Figure 7

Effect of NMDA receptor antagonists on glycine and D-serine-activated currents in astrocytes. (A) Representative responses activated in acutely-isolated cortical astrocytes by consecutive application of 50 μM NMDA (no glycine added) and 10 μM glycine in control and the presence of 10 μM MK801. NMDA and glycine were applied in turn with a 2 min interval. The gradual decline of the astrocytic response is indicative of a use-dependent block; block by MK801 established after the fourth to fifth round of application. Note the synchronous decrease in the amplitude of both NMDA and glycine-activated currents. (B) Representative responses activated in acutely-isolated cortical astrocytes by consecutive applications of 50 μM NMDA (no glycine added) and 10 μM D-serine in control and after the application of 10 μM memantine. NMDA and D-serine were applied in turn with a 2 min interval. (C) Pooled data (mean ± SD for five astrocytes) on the inhibitory effect of MK801, memantine and UBP141 on astrocytic responses. Although glycine-activated currents were less sensitive to the antagonists than the NMDA-activated currents, the difference was not statistically significant. All recordings were made at a holding potential of −80 mV in the presence of picrotoxin and strychnine.

potentiation of NMDA-activated currents by D-serine (Figure 6), not desensitization, which is not expected for GluN1/GluN3 assembly (Henson *et al.*, 2010). Furthermore, both NMDA-activated currents and responses to glycine and D-serine were strongly inhibited by D-AP5 (Lalo *et al.*, 2006), memantine (Figures 2,3) and MK-801 (Figures 4 and 7). Thus, the pharmacological profile of NMDA-mediated responses in cortical astrocytes cannot be purely attributed to di-heteromeric GluN1/GluN3 receptors.

The only structural composition that can explain all the pharmacological and functional properties of the astroglial NMDA receptors we describe here is a tri-heteromer incorporating, in addition to two GluN1 subunits, one GluN2C or D subunit and one GluN3 subunit, rendering the astroglial receptors much less sensitive to Mg^{2+} but sensitive to UBP141, memantine and D-AP5 (Figures 1, 3 and 7). This suggestion is supported by the weak Mg^{2+} block observed for tri-heteromeric GluN1/GluN2/GluN3 receptors (Sasaki *et al.*, 2002; Tong *et al.*, 2008). It is also in line with evidence for the expression of GluN2C, GluN2D and GluN3 subunits in white matter oligodendrocytes (Karadottir *et al.*, 2005; Burzomato *et al.*, 2010).

It is worth noting that astroglial NMDARs showed lower sensitivity to Mg^{2+} block than GluN1/GluN2C/GluN3A receptors in oligodendrocytes (Karadottir *et al.*, 2005; Burzomato *et al.*, 2010). This might be explained by the incorporation of different splice variants of GluN1 and GluN2 subunits and/or incorporation of GluN3B subunit. It has been shown that the co-assembly of GluN3 with different splice variants of the GluN1 subunit can affect the functional properties of di-heteromeric receptors (Cavara *et al.*, 2009; Smothers and Woodward, 2009). In particular, the fraction of the glycine-activated current blocked by Mg^{2+} in the receptor complexes assembled with GluN1-2b and GluN1-3b were much lower than in the receptors containing other GluN1 variants (Cavara *et al.*, 2009). Furthermore, the degree of the Mg^{2+} block of almost all isoforms of GluN1/GluN3B receptors (Cavara *et al.*, 2009) was lower than the Mg^{2+} block reported for GluN1/GluN3A receptors (Chatterton *et al.*, 2002). Recently, it has been reported that splicing of the GluN2A subunit can lead to loss of Mg^{2+} block (Endele *et al.*, 2010). Thus, it is speculated that co-assembly of GluN3A or GluN3B with different variants of GluN1 and GluN2 subunits might result in tri-heteromeric receptors with different sensitivities to Mg^{2+}.

Whatever the particular mechanism is that explains the variance in the Mg^{2+} sensitivity conferred by GluN3 subunits to glial triplet receptors, Mg^{2+} sensitivity is weak both in astrocytes and oligodendrocytes. This may have similar physiological consequences: glial NMDA receptors can be activated at physiological resting potentials and bring significant contribution to glial Ca^{2+} signalling despite their reduced Ca^{2+} permeability. In view of the possible implication of GluN3-containing receptors in brain injuries (Henson *et al.*, 2010), the molecular structure of glial NMDA receptors is worth investigating further.

The other important finding of the present study is the difference in the affinity of glial and neuronal NMDA receptors to memantine at physiological concentrations of Mg^{2+}. The recent successes of memantine in the treatment of Alzheimer's disease has revived interest in the therapeutic use of NMDA antagonists (Lipton, 2006). Our findings strongly support the conclusions of Kotermanski and Johnson (2009), that neuronal NMDA receptors can have a much lower affinity for memantine in physiological conditions than was previously thought, and that the clinical effects of therapeutic doses of memantine are most likely to be related to its effect on GluN2C/D- rather than on GluN2A/B-containing receptors. Furthermore, our results suggest that those GluN2C and D subunits, which might underlie the therapeutic effects of memantine, may be mediated via astroglial NMDA receptors.

We have shown that the substantial differences in the pharmacological and biophysical properties of astroglial and neuronal NMDA receptors enables the selective modulation of synaptically-driven astrocytic signalling. This may be very useful for elucidating the mechanisms of neuron-glia communications and the development of novel therapeutic agents specifically targeting glial signalling.

Acknowledgements

This work was supported by a grant from BBSRC UK (BB/F021445; Y.P.). The authors thank Prof B. Frenguelli and Prof N. Dale for early discussion and helpful comments on the manuscript.

Conflicts of interest

On behalf of the authors, I confirm that there is no potential conflict of interest.

References

Agulhon C, Petravicz J, McMullen AB, Sweger EJ, Minton SK, Taves SR *et al.* (2008). What is the role of astrocyte calcium in neurophysiology? Neuron 59: 932–946.

Bergles DE, Jabs R, Steinhauser C (2009). Neuron-glia synapses in the brain. Brain Res Rev 63: 130–137.

Brothwell SL, Barber JL, Monaghan DT, Jane DE, Gibb AJ, Jones S (2008). NR2B- and NR2D-containing synaptic NMDA receptors in developing rat substantia nigra pars compacta dopaminergic neurones. J Physiol 586: 739–750.

Burnashev N, Villarroel A Sakmann B (1996). Dimensions and ion selectivity of recombinant AMPA and kainate receptor channels and their dependence on Q/R site residues. J Physiol Lond 496: 165–173.

Burzomato V, Frugier G, Perez-Otano I, Kittler JT, Attwell D (2010). The receptor subunits generating NMDA receptor mediated currents in oligodendrocytes. J Physiol 588: 3403–3414.

Castro NG, Albuquerque EX (1995). alpha-Bungarotoxin-sensitive hippocampal nicotinic receptor channel has a high calcium permeability. Biophys J 68: 516–524.

Cavara NA, Hollmann M (2008). Shuffling the deck anew: how NR3 tweaks NMDA receptor function. Mol Neurobiol 38: 16–26.

Cavara NA, Orth A, Hollmann M (2009). Effects of NR1 splicing on NR1/NR3B-type excitatory glycine receptors. BMC Neurosci 10: 32–42.

Chatterton JE, Awobuluyi M, Premkumar LS, Takahashi H, Talantova M, Shin Y *et al.* (2002). Excitatory glycine receptors containing the NR3 family of NMDA receptor subunits. Nature 415: 793–798.

Cull-Candy SG, Leszkiewicz DN (2004). Role of distinct NMDA receptor subtypes at central synapses. Sci STKE 2004: re16.

Danbolt NC (2001). Glutamate uptake. Prog Neurobiol 65: 1–105.

Endele S, Rosenberger G, Geider K, Popp B, Tamer C, Stefanova I *et al.* (2010). Mutations in GRIN2A and GRIN2B encoding regulatory subunits of NMDA receptors cause variable neurodevelopmental phenotypes. Nat Genet 42: 1021–1026.

Erreger K, Geballe MT, Kristensen A, Chen PE, Hansen KB, Lee CJ *et al.* (2007). Subunit-specific agonist activity at NR2A-, NR2B-, NR2C-, and NR2D-containing N-methyl-D-aspartate glutamate receptors. Mol Pharmacol 72: 907–920.

Evans RJ, Lewis C, Virginio C, Lundstrom K, Buell G, Surprenant A *et al.* (1996). Ionic permeability of, and divalent cation effects on, two ATP-gated cation channels (P2X receptors) expressed in mammalian cells. J Physiol 497 (Pt 2):413–422.

Fucile S (2004). Ca2+ permeability of nicotinic acetylcholine receptors. Cell Calcium 35: 1–8.

Furukawa H, Singh SK, Mancusso R, Gouaux E (2005). Subunit arrangement and function in NMDA receptors. Nature 438: 185–192.

Henson MA, Roberts AC, Perez-Otano I, Philpot BD (2010). Influence of the NR3A subunit on NMDA receptor functions. Prog Neurobiol 91: 23–37.

Hu WH, Walters WM, Xia XM, Karmally SA, Bethea JR (2003). Neuronal glutamate transporter EAAT4 is expressed in astrocytes. Glia 44: 13–25.

Iino M, Ozawa S, Tsuzuki K (1990). Permeation of calcium through excitatory amino acid receptor channels in cultured rat hippocampal neurones. J Physiol 424: 151–165.

Isa T, Itazawa S, Iino M, Tsuzuki K Ozawa S (1996). Distribution of neurones expressing inwardly rectifying and $Ca2^{+}$permeable AMPA receptors in rat hippocampal slices. J Physiol Lond 491: 719–733.

Karadottir R, Cavelier P, Bergersen LH, Attwell D (2005). NMDA receptors are expressed in oligodendrocytes and activated in ischaemia. Nature 438: 1162–1166.

Kotermanski SE, Johnson JW (2009). Mg2+ imparts NMDA receptor subtype selectivity to the Alzheimer's drug memantine. J Neurosci 29: 2774–2779.

Krebs C, Fernandes HB, Sheldon C, Raymond LA, Baimbridge KG (2003). Functional NMDA receptor subtype 2B is expressed in astrocytes after ischemia in vivo and anoxia in vitro. J Neurosci 23: 3364–3372.

Lalo U, Pankratov Y, Kirchhoff F, North RA, Verkhratsky A (2006). NMDA receptors mediate neuron-to-glia signaling in mouse cortical astrocytes. J Neurosci 26: 2673–2683.

Lalo U, Pankratov Y, Wichert SP, Rossner MJ, North RA, Kirchhoff F *et al.* (2008). P2X1 and P2X5 subunits form the functional P2X receptor in mouse cortical astrocytes. J Neurosci 28: 5473–5480.

Lewis CA (1979). Ion-concentration dependence of the reversal potential and single cell conductance of ion channel at the frog neuromuscular junction. J Physiol (Lond) 286: 417–445.

Lipton SA (2006). NMDA receptors, glial cells, and clinical medicine. Neuron 50: 9–11.

Matsuda K, Fletcher M, Kamiya Y, Yuzaki M (2003). Specific assembly with the NMDA receptor 3B subunit controls surface expression and calcium permeability of NMDA receptors. J Neurosci 23: 10064–10073.

Matsui K, Jahr CE (2004). Differential control of synaptic and ectopic vesicular release of glutamate. J Neurosci 24: 8932–8939.

Matute C, Domercq M, Sanchez-Gomez MV (2006). Glutamate-mediated glial injury: mechanisms and clinical importance. Glia 53: 212–224.

Mayer ML, Westbrook GL (1987). Permeation and block of N-methyl-D-aspartic acid receptor channels by divalent cations in mouse cultured central neurones. J Physiol 394: 501–527.

Micu I, Jiang Q, Coderre E, Ridsdale A, Zhang L, Woulfe J *et al*. (2006). NMDA receptors mediate calcium accumulation in myelin during chemical ischaemia. Nature 439: 988–992.

Monyer H, Burnashev N, Laurie DJ, Sakmann B, Seeburg PH (1994). Developmental and regional expression in the rat brain and functional properties of four NMDA receptors. Neuron 12: 529–540.

Morley RM, Tse HW, Feng B, Miller JC, Monaghan DT, Jane DE (2005). Synthesis and pharmacology of N1-substituted piperazine-2,3-dicarboxylic acid derivatives acting as NMDA receptor antagonists. J Med Chem 48: 2627–2637.

Nolte C, Matyash M, Pivneva T, Schipke CG, Ohlemeyer C, Hanisch UK *et al*. (2001). GFAP promoter-controlled EGFP-expressing transgenic mice: a tool to visualize astrocytes and astrogliosis in living brain tissue. Glia 33: 72–86.

Pankratov Y, Lalo U, Krishtal O, Verkhratsky A (2002). Ionotropic P2X purinoreceptors mediate synaptic transmission in rat pyramidal neurones of layer II/III of somato-sensory cortex. J Physiol 542: 529–536.

Paoletti P, Neyton J (2007). NMDA receptor subunits: function and pharmacology. Curr Opin Pharmacol 7: 39–47.

Qian A, Johnson JW (2006). Permeant ion effects on external Mg2+ block of NR1/2D NMDA receptors. J Neurosci 26: 10899–10910.

Sasaki YF, Rothe T, Premkumar LS, Das S, Cui J, Talantova MV *et al*. (2002). Characterization and comparison of the NR3A subunit of the NMDA receptor in recombinant systems and primary cortical neurons. J Neurophysiol 87: 2052–2063.

Schipke CG, Ohlemeyer C, Matyash M, Nolte C, Kettenmann H, Kirchhoff F (2001). Astrocytes of the mouse neocortex express functional N-methyl-D-aspartate receptors. Faseb J 15: 1270–1272.

Smothers CT, Woodward JJ (2009). Expression of glycine-activated diheteromeric NR1/NR3 receptors in human embryonic kidney 293 cells Is NR1 splice variant-dependent. J Pharmacol Exp Ther 331: 975–984.

Steinert JR, Postlethwaite M, Jordan MD, Chernova T, Robinson SW, Forsythe ID (2010). NMDAR-mediated EPSCs are maintained and accelerate in time course during maturation of mouse and rat auditory brainstem in vitro. J Physiol 588: 447–463.

Tong G, Takahashi H, Tu S, Shin Y, Talantova M, Zago W *et al*. (2008). Modulation of NMDA receptor properties and synaptic transmission by the NR3A subunit in mouse hippocampal and cerebrocortical neurons. J Neurophysiol 99: 122–132.

Wrighton DC, Baker EJ, Chen PE, Wyllie DJ (2008). $Mg2^{+}$ and memantine block of rat recombinant NMDA receptors containing chimeric NR2A/2D subunits expressed in Xenopus laevis oocytes. J Physiol 586: 211–225.